

The behaviour of quiescent accretion discs in dwarf novae

M. R. Truss¹, G.A. Wynn² and P.J. Wheatley²

¹ *School of Physics and Astronomy, University of St Andrews, North Haugh, St Andrews, Fife, KY16 9SS, Scotland, UK*

² *Department of Physics and Astronomy, University of Leicester, University Road, Leicester, LE1 7RH, UK*

11 December 2018

ABSTRACT

We propose a simple explanation for the constant mean brightness observed between outbursts in dwarf novae. Secular changes in the total energy dissipation rate of the accretion disc brought about by variations in surface density, temperature and disc radius can be regulated by the gradual cooling of a small, critically-stable hot inner region. The hypothesis is supported with two-dimensional time-dependent numerical models of dwarf nova accretion discs.

Key words: accretion, accretion discs - instabilities - binaries: close - methods: numerical - novae, cataclysmic variables.

1 INTRODUCTION

Dwarf novae have been observed extensively since the discovery of U Geminorum in the mid-nineteenth century. They account for well over half of the non-magnetic cataclysmic variables (Ritter & Kolb 1998), and consist of a white dwarf accreting from a low-mass star via Roche lobe overflow. The dwarf novae are observed in two states: a quiescent, almost constant-luminosity low state that may last for months, and a regular (but aperiodic) high luminosity, outburst state lasting for several days. The transition between the states is fairly rapid; typically the V magnitude changes by four magnitudes over the course of a day or so.

The outbursts are attributed to a thermal-viscous instability in the accretion disc, often referred to as the disc instability, which is associated with the steep dependence of opacity with temperature at the point where hydrogen begins to ionize ($T_H \sim 6500$ K). Our understanding of the physical properties of the accretion disc in quiescence is less complete. In particular, while great strides have been made in the identification of a magneto-rotational instability (MRI) responsible for the transport of angular momentum (Balbus & Hawley 1991), the efficiency of this instability is sensitive to the degree of ionization in the accretion disc (Matsumoto & Tajima 1995). It remains unclear whether the MRI can sustain the necessary angular momentum transport appropriate to a cool, quiescent disc. It is possible that other viscosity mechanisms are at work in quiescence (Menou 2000).

There have been several rigorous one-dimensional calculations of dwarf nova outbursts within the framework of the disc instability model (Smak (1984b); Ichikawa & Osaki (1992); Hameury et al. (1998) and many others). The recent review of Lasota (2001) describes the current state of the disc instability model, and contains an excellent commentary on its scope and limitations. In his review, Lasota describes quiescence as ‘the Achilles’ heel’ of the model, because the model handles the behaviour of dwarf novae in quiescence rather poorly. One of the major prob-

lems with the numerical models has been that when the correct boundary conditions are used (in particular an outer disc radius that is not constrained to be fixed) the models are unable to reproduce the observed constant level of brightness during quiescence. The brightness almost always increases between the outbursts.

Visual observations of dwarf novae by amateur astronomers cover more than a century in some cases and decades in many others (for example Cannizzo & Mattei (1992)). These visual observations show scatter at the level of 0.5 to 1 magnitudes, so it is difficult to see short-term variations, but it is clear that the mean visible flux remains approximately constant throughout quiescence. In contrast, disc instability models consistently predict an increasing brightness during quiescence. The amplitude of the predicted increase lies in the range 1 to 3 magnitudes, and would certainly have been observed if present.

In this paper we suggest an explanation for this discrepancy. In the next section we present an analytic model of how the viscous energy generation rate responds to variations in the physical state of the disc over the quiescent interval in a dwarf nova. We show that in a disc with a constant Shakura-Sunyaev viscosity, the total viscous energy dissipation rate increases in response to the expected changes in surface density, temperature and outer disc radius. However, we show that it is possible for the total viscous energy generation rate to remain constant if there is a small portion of the disc that remains in the high-viscosity state during quiescence. This hypothesis is supported by two-dimensional smoothed particle hydrodynamics (SPH) simulations of accretion discs in Section 3, which incorporate the evolution of the free outer disc boundary in response to the full two-dimensional tidal potential of the binary. We discuss the possible implications for the disc instability model in Section 4.

2 QUIESCENT LUMINOSITY

We consider the local viscous energy dissipation rate in an accretion disc, which is given by

$$D(r, t) = \frac{9}{4} \nu(t) \Sigma(r, t) \frac{GM_1}{r(t)^3}. \quad (1)$$

This definition differs by a factor of two from that which appears in some treatments. Here we express the local dissipation rate integrated over the vertical interval $-\infty \leq z \leq \infty$, not just from the mid-plane. We assume that the viscosity can be described by the α prescription of Shakura & Sunyaev (1973):

$$\nu = \alpha c_s H = \alpha c_s^2 \left(\frac{r^3}{GM_1} \right)^{\frac{1}{2}}, \quad (2)$$

where the viscosity parameter α is a dimensionless constant.

Now, at a time t , the total luminosity due to viscous energy dissipation in the accretion disc is

$$L(t) = \int_{R_{\text{in}}}^{R_{\text{d}}} D(r, t) 2\pi r dr, \quad (3)$$

where R_{in} and R_{d} are the inner and outer radii of the disc. Then,

$$L(t) \propto \int_{R_{\text{in}}}^{R_{\text{d}}} \alpha T(r, t) \Sigma(r, t) r(t)^{-\frac{1}{2}} dr, \quad (4)$$

where $T(r, t)$ is the local mid-plane temperature at time t .

Since the conditions in the accretion disc are not steady during quiescence, there is no exact analytic expression for the time-dependent evolution of the surface density, $\Sigma(r, t)$ and the mid-plane temperature, $T(r, t)$. However, we do know that these quantities must increase during quiescence if another outburst is to follow via disc instability. Indeed, given that the critical surface densities for triggering and suppressing the disc instability vary almost linearly with radius (Cannizzo et al. 1988), one could envisage a model in which the surface density profile remains linear with radius while its gradient or mean level steadily increases. Further, we could assume that the radial temperature profile remains almost flat during quiescence, as suggested by eclipse mapping of the dwarf nova Z Cha (Wood et al. 1986). We do not make these assumptions, but for simplicity we express the product

$$T(r, t) \Sigma(r, t) = A(t) r^n \quad (5)$$

where A is independent of radius and n can take any value. Under the two assumptions discussed above, n would be unity, but we keep it as a free parameter to take into account other possibilities. Its exact value (positive or negative) does not affect our argument here, but we do assume that since temperature and surface density increase during quiescence, the quantity $dA/dt > 0$. In this case,

$$L(t) \propto \alpha_c A(t) \left[R_{\text{d}}^{n+\frac{1}{2}} - R_{\text{in}}^{n+\frac{1}{2}} \right], \quad (6)$$

where the entire disc is on the cool branch of the disc instability curve, with a viscosity parameter α_c . If we consider how the luminosity will vary during quiescence, assuming that the inner radius remains constant,

$$\frac{dL}{dt} \propto \alpha_c \left[\left(R_{\text{d}}^{n+\frac{1}{2}} - R_{\text{in}}^{n+\frac{1}{2}} \right) \frac{dA}{dt} + \left(n + \frac{1}{2} \right) A R_{\text{d}}^{n-\frac{1}{2}} \frac{dR_{\text{d}}}{dt} \right]. \quad (7)$$

The disc radius is expected to decrease slowly between dwarf nova outbursts, since the accretion rate onto the primary is small

and material with low specific angular momentum is accumulating near the outer edge from the gas stream. This has been confirmed by one-dimensional disc instability calculations (Smak 1984a; Ichikawa & Osaki 1992). However, this term is dominated by the increasing surface density and temperature, and the total disc luminosity increases between outbursts.

Now consider a disc with two regions: a hot, inner region on the upper branch of the instability curve with α_{h} , and a cool outer region as before. We term the transition radius between the regions R_{t} . In this case,

$$L(t) \propto \int_{R_{\text{in}}}^{R_{\text{t}}} \alpha_{\text{h}} A_{\text{h}}(t) r^{n-\frac{1}{2}} dr + \int_{R_{\text{t}}}^{R_{\text{d}}} \alpha_{\text{c}} A_{\text{c}}(t) r^{n-\frac{1}{2}} dr, \quad (8)$$

or

$$L(t) \propto \left[(\alpha_{\text{h}} A_{\text{h}} - \alpha_{\text{c}} A_{\text{c}}) R_{\text{t}}^{n+\frac{1}{2}} + \alpha_{\text{c}} A_{\text{c}} R_{\text{d}}^{n+\frac{1}{2}} - \alpha_{\text{h}} A_{\text{h}} R_{\text{in}}^{n+\frac{1}{2}} \right]. \quad (9)$$

Now,

$$\begin{aligned} \frac{dL}{dt} \propto & \left[\left(n + \frac{1}{2} \right) (\alpha_{\text{h}} A_{\text{h}} - \alpha_{\text{c}} A_{\text{c}}) R_{\text{t}}^{n-\frac{1}{2}} \frac{dR_{\text{t}}}{dt} \right. \\ & + \left(n + \frac{1}{2} \right) \alpha_{\text{c}} A_{\text{c}} R_{\text{d}}^{n-\frac{1}{2}} \frac{dR_{\text{d}}}{dt} \\ & + \alpha_{\text{h}} \left(R_{\text{t}}^{n+\frac{1}{2}} - R_{\text{in}}^{n+\frac{1}{2}} \right) \frac{dA_{\text{h}}}{dt} \\ & \left. + \alpha_{\text{c}} \left(R_{\text{d}}^{n+\frac{1}{2}} - R_{\text{t}}^{n+\frac{1}{2}} \right) \frac{dA_{\text{c}}}{dt} \right]. \quad (10) \end{aligned}$$

The second and fourth terms of this equation are identical to the two terms in equation 7; however, there are now two additional terms involving the rate of change in R_{t} and A_{h} . The presence of a hot inner region means that there are more parameters available to change dL/dt . As an example, the coefficients of the two new terms in equation 10 involve the hot-state viscosity, α_{h} , while the coefficients of the other terms involve only α_{c} . Since we expect $\alpha_{\text{h}} \sim 10\alpha_{\text{c}}$ in a dwarf nova accretion disc, any changes in dissipation rate brought about by the evolution of the cool part of the disc could be offset by much smaller changes in the hot, inner region.

We stress that the above analysis is in no way meant to be a self-consistent solution of the accretion flow. We simply demonstrate that a hot, high-viscosity inner region provides many more avenues for evolution of the disc. For example, the situation is complicated by the fact that we do not know the correct value of n or the correct form of $A(t)$. In particular, it is extremely difficult to predict the response of R_{d} and R_{t} in a non-steady accretion disc. It is only in a numerical calculation that these effects can be studied in more detail.

In the next section, we demonstrate the effect of maintaining a hot, high-viscosity inner region with two-dimensional smoothed particle hydrodynamics calculations of accretion discs in dwarf novae.

3 TWO-DIMENSIONAL SPH CALCULATIONS

3.1 Numerical method

We use a two-dimensional (2D) smoothed particle hydrodynamics scheme to model the evolution of an accretion disc in a close binary. The model includes the full tidal potential due to the secondary star

and has been discussed in detail and tested with reference to dwarf novae in Truss et al. (2000).

SPH uses an ensemble of particles to describe a fluid. The advantages of such a Lagrangian scheme to model these systems immediately becomes apparent: the response of the free outer boundary of the accretion disc to the mass stream and the tidal potential are treated in a self-consistent manner. For a wider discussion of SPH, the reader is referred to the review of Monaghan (1992).

We solve the SPH momentum equation in the Lagrangian (co-moving) frame, with an artificial viscosity parameter ζ for each particle, i , such that

$$\frac{d\mathbf{v}_i}{dt} = - \sum_j m_j \left(\frac{P_i}{\rho_i^2} + \frac{P_j}{\rho_j^2} - \frac{\zeta \bar{c}_{ij} \mu_{ij}}{\bar{\rho}_{ij}} \right) \nabla_i W_{ij} \quad (11)$$

where $\bar{\rho}_{ij}$ and \bar{c}_{ij} are the average density and sound speed of a pair of particles i and j respectively, W_{ij} is an interpolating kernel (here taken to be a cubic spline) and

$$\mu_{ij} = \frac{H \mathbf{v}_{ij} \cdot \mathbf{r}_{ij}}{\mathbf{r}_{ij}^2 + \eta^2}. \quad (12)$$

The softening parameter η avoids singularities and H is the length scale over which the viscous energy is dissipated. Here, this is set to the scale height, $H = \frac{c_s}{\Omega}$. We do not use a viscosity term that is quadratic in μ_{ij} , often denoted by the parameter β in SPH equations. A linear term is quite sufficient in this case. Murray (1996) has shown that in 2D, the ζ term introduces a shear viscosity

$$\nu = \frac{1}{8} \zeta c_s H, \quad (13)$$

so the implementation is equivalent to a Shakura-Sunyaev viscosity of $\alpha = \zeta/8$. We also solve the thermal energy equation

$$\frac{du_i}{dt} = \frac{1}{2} \sum_{j=1}^N m_j \left[\frac{P_i}{\rho_i^2} + \frac{P_j}{\rho_j^2} - \frac{\zeta \mu_{ij} \bar{c}_{ij}}{\bar{\rho}_{ij}} \right] (\mathbf{v}_i - \mathbf{v}_j) \cdot \nabla_i W_{ij}. \quad (14)$$

The thermal-viscous instability is incorporated using a viscosity switch for each particle based on the local surface density. The critical conditions for the triggering or suppression of the instability are roughly linear in radius (Cannizzo et al. 1988). Here, we take

$$\Sigma_{\max} = C_{\text{hot}} \frac{R}{a}; \quad \Sigma_{\min} = C_{\text{cold}} \frac{R}{a}, \quad (15)$$

where C_{hot} and C_{cold} are constants and a is the binary separation. If the surface density of a particle exceeds Σ_{\max} , then its viscosity is increased smoothly from a value ζ_c to a value ζ_h on a 'thermal' time-scale τ_{trigger} , where $\tau_{\text{trigger}} \ll t_{\text{viscous}}$. Its viscosity remains high until the local surface density falls below Σ_{\min} , when it is returned to ζ_c on a similar time-scale. In contrast to previous implementations of this code which were fully isothermal, here we change the sound speed of the gas whenever the critical surface density thresholds are crossed. The change in sound speed from a value c_{low} to a value c_{high} (and vice versa) is made on precisely the same time-scale as the change in viscosity parameter. Hence, no scaling is required for the amplitude of the luminosity variations driven by viscous dissipation in the disc.

3.2 Simulations

We perform simulations of an accretion disc in a binary stellar system with the parameters of the dwarf nova IP Pegasi taken from the catalogue of Ritter & Kolb (1998): $P_{\text{orb}} = 0.158$ d, $M_1 = 1.15 M_{\odot}$ and $M_2 = 0.67 M_{\odot}$. The accretion disc is built

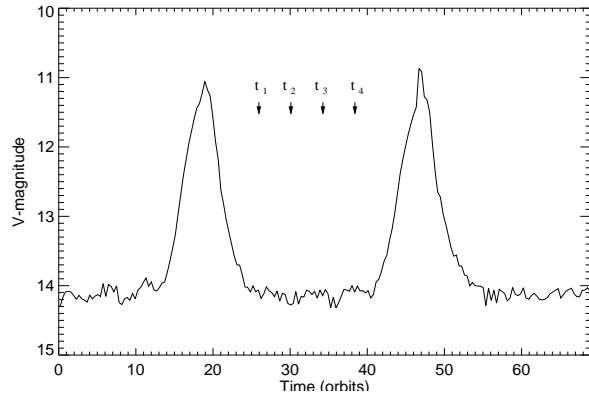


Figure 1. V-band light curve for a simulation of the dwarf nova IP Peg. Here, the inner part of the disc remains in the hot, high viscosity state throughout the quiescent intervals. The size of the hot region varies during quiescence, leading to the small variations in the light curve, but keeping the mean quiescent level flat. The four times t_1 to t_4 are defined in the caption of Figure 2.

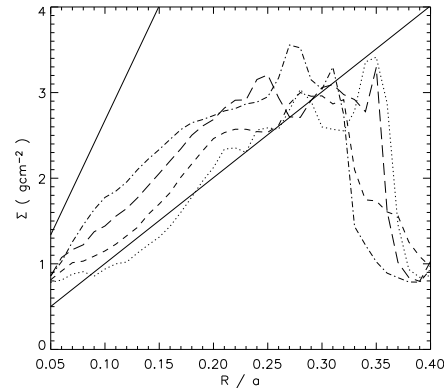


Figure 2. Evolution of surface density in the accretion disc during quiescence in the first simulation. The curves correspond to the following times in Figure 1: $t_1=26$ (dots), $t_2=30$ (dashes), $t_3=34$ (long dashes) and $t_4=38$ (dot-dashes). The solid straight lines show the critical surface densities used in the simulation.

up from scratch using a stream of particles injected from the inner Lagrangian point at a constant rate of $10^{-10} M_{\odot} \text{yr}^{-1}$. We use $C_{\text{hot}} = 18.7 \text{ g cm}^{-2}$, $C_{\text{cold}} = 7.02 \text{ g cm}^{-2}$, $\tau_{\text{trigger}} = 1750 \text{ s}$, viscosity parameters $\zeta_c = 1$ and $\zeta_h = 10$, corresponding to $\alpha_c = 0.125$ and $\alpha_h = 1.25$, and sound speeds $c_{\text{low}} = 0.05 a \Omega_b$ and $c_{\text{high}} = 0.15 a \Omega_b$.

Figure 1 shows the resulting V-band light curve. The light curve is calculated under the assumption that the disc is optically thick and each annulus of gas radiates as a black body. The Planck function is integrated over the interval 500 to 600 nm and summed over the annuli. In this simulation, many particles in the inner part of the disc remain constantly in the hot, high-viscosity state. In this region the critical surface densities given in the equations 15 are both low and close together. The overall mean brightness is roughly constant during quiescence, with small variations occurring as the size of the hot region changes. It can be seen that this behaviour is now consistent with that observed in dwarf in quiescence. Our predicted variability in quiescence has too small an amplitude to be detected the visual light curves of amateur astronomers, but it is

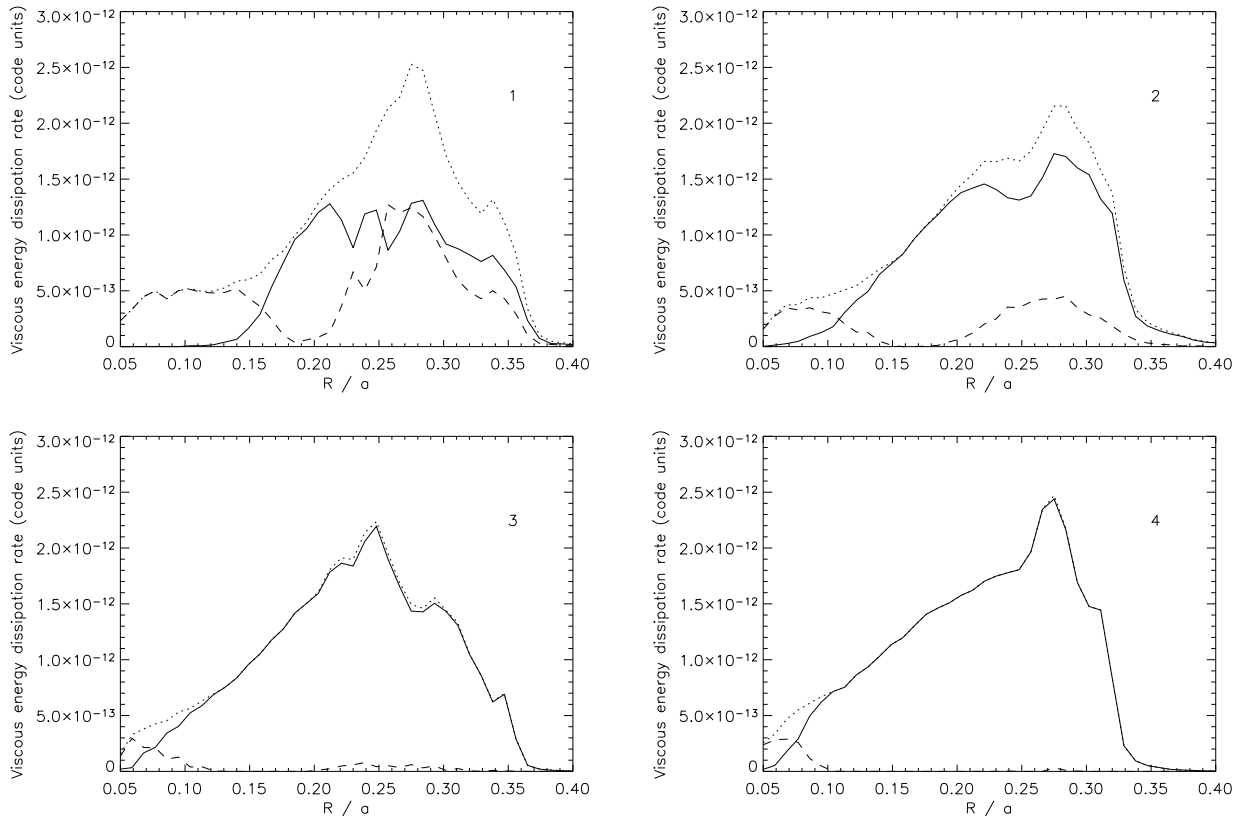


Figure 3. Evolution of the contributions to the viscous energy dissipation rate made by the high and low viscosity particles in the disc for each of the times t_1 (top left) to t_4 (lower right). The solid curve shows the contribution from low viscosity particles ($\zeta \leq 1.5$), the dashed curve shows the contribution from high viscosity particles ($\zeta > 1.5$), and the dotted curve the total viscous energy dissipation rate. The increasing low-viscosity contribution is offset by a decrease in the contribution from the high viscosity particles.

strikingly similar to that observed in the few detailed CCD observations of dwarf novae in quiescence (see, for example Wagner et al. (1998)).

Figure 2 shows the variation in surface density during one of the quiescent intervals. It can be seen that the surface density in the inner disc never drops below Σ_{min} and hence remains in the hot state throughout quiescence.

A hot inner disc seems to be a natural feature of these simulations, and in fact is a natural consequence of the linear triggers that get progressively closer together in the inner disc. With triggers of this form it is difficult to see how the inner regions of the disc can avoid entering the high state during quiescence. It is not immediately obvious to us why this is not a feature seen in one-dimensional models.

The response of the disc is shown in more detail in Figure 3, which shows the evolving contributions to the local viscous energy dissipation rate of the low and high viscosity particles at each radius in the disc. For the purposes of this figure we define the high viscosity particles as those with $\zeta > 1.5$, to distinguish between those particles with a genuinely low viscosity, such as those arriving from the stream which all have $\zeta = 1.0$, and those which may be changing viscosity from a recent high state. At the beginning of quiescence, when the surface density and dissipation rate in the outer disc are low, the high viscosity particles dominate the inner disc. The hot particles at large radii ($R > 0.2a$) in panels 1 and 2 remain from the previous outburst. By mid-quiescence (panel 3), they

have cooled completely and the outer disc is dominated by the cold particles arriving from the mass stream. As the cold, outer regions begin to refill, the corresponding increase in dissipation is offset by a decrease in the size of the residual high viscosity inner region. An estimate for the transition radius, R_h , can be made from the intersection of the solid and dashed curves in Figure 3. Although R_h is varying both up and down during quiescence, the general trend is a decrease from $R_h \sim 0.15a$ in panel 1, to $R_h \sim 0.08a$ in panel 4.

Throughout the quiescence, the outer radius shrinks slightly, in accordance with the expectations discussed in Section 2. We find that over the course of quiescence, although the mean luminosity remains constant, the total disc mass increases by 19 %, which is comparable to the mass accreted by the primary in each outburst.

A second simulation of IP Peg was performed in order to demonstrate that it is the hot inner parts that keep the mean quiescent brightness constant. In this case, we used critical surface densities that did not have a linear radial dependence, but were constant: $\Sigma_{max} = C_{up}$ and $\Sigma_{min} = C_{down}$, where we used $C_{up} = 4.1 \text{ g cm}^{-2}$ and $C_{down} = 1.6 \text{ g cm}^{-2}$. In this case, it is more unlikely that the surface density of the disc in the inner parts can reach the critical level during quiescence, so the inner part of the disc remains in the cool, low-viscosity state.

Figures 4 and 6 show the resulting V-band light curve and variations in surface density during the second simulation. The outbursts are almost identical in profile, and the more familiar solution

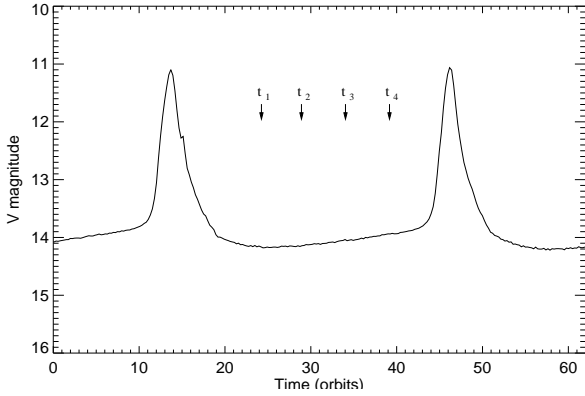


Figure 4. In this simulation of outbursts in IP Peg, the surface density trigger for the disc instability in the inner part of the disc is raised so that this region cannot reach the hot, high viscosity state during quiescence. Consequently, the mean brightness level rises steadily between outbursts. The four times t_1 to t_4 are defined in the caption of Figure 6.

is recovered, with a mean quiescent level that steadily increases between the outbursts as gas accumulates in the disc.

The increase in V-magnitude during quiescence ($\sim 0.2 - 0.3$ mag.) is smaller than the increase seen in 1-d models (~ 1 mag.). This can be understood in terms of the sound speed, which only changes (that is, the disc only heats up) when the viscosity changes. In the 1-d models, the temperature and sound speed of the disc increase during quiescence as the surface density increases, even when $\alpha = \alpha_{\text{cold}}$ everywhere. It is trivial to estimate the effect that this change in sound-speed would have on our simulation. The dissipation rate, $D(r) \sim \nu \Sigma \sim T_c \Sigma$, where T_c is the mid-plane temperature. In our simulation, the dissipation rate at the end of quiescence is about 1.25 times (0.2 magnitudes larger than) the rate at the beginning of quiescence. This arises from the increase in surface density alone. Given a reasonable increase of a factor of two in T_c over quiescence, the increase in dissipation rate would be a factor of two higher, that is a difference of 2.5 times (or 1 magnitude). Indeed, we can go one step further and incorporate this into the simulations.

In an α -disc, surface density scales with sound speed as $\Sigma \sim c_s^{3/14}$. For all particles with $\alpha = \alpha_c$, we let

$$c_s = c_{\text{low}} \left(\frac{\Sigma}{\Sigma_{\text{min}}} \right)^{\frac{3}{14}}. \quad (16)$$

The results can be seen in Figure 5. For the flat-trigger case (simulation 2), where most of the particles during quiescence have $\alpha = \alpha_{\text{cold}}$, the rise in the V-band light curve is now a full magnitude, in line with our expectations. The difference in simulation 1 is much less marked, because there the viscosity is not α_{cold} everywhere during quiescence. The amplitude of the variations in quiescence in the first simulation remain much smaller than the increase in V-band magnitude in the second simulation.

Figure 7 shows the evolution of total viscous energy generation over the disc in the second simulation. Again, the outer radius moves inward slightly, but there is a general increase in dissipation rate at all radii. The increase in disc mass is virtually identical to that found in simulation 1, around 19%.

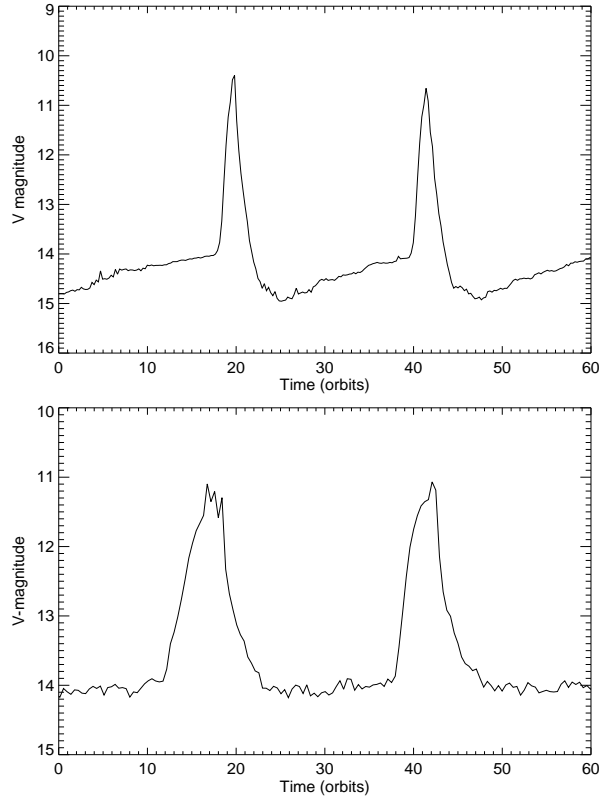


Figure 5. Evolution of the V-band light curve when the sound speed is varied with surface density for the cold particles. Top: the light curve of the second (flat-trigger) simulation now shows a brightening by a full magnitude in quiescence. Bottom: the difference in the first simulation is much less marked.

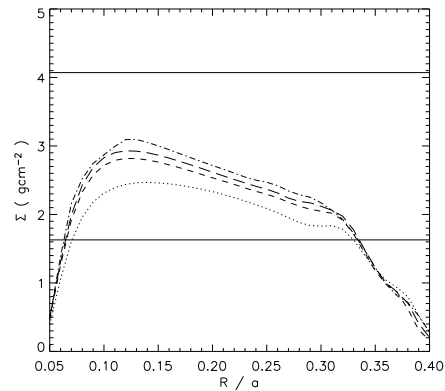


Figure 6. Evolution of surface density in the accretion disc during quiescence in the second simulation. The curves correspond to the following times in Figure 4: $t_1=24$ (dots), $t_2=29$ (dashes), $t_3=34$ (long dashes) and $t_4=39$ (dot-dashes). The solid straight lines show the critical surface densities used in the simulation.

4 DISCUSSION

We have shown that the observed constant mean brightness of dwarf novae during quiescence can be regulated by the response of a small inner portion of the disc that remains in a high-viscosity state close to the critical surface density limits for the thermal-viscous disc instability. Over the course of quiescence, the increase

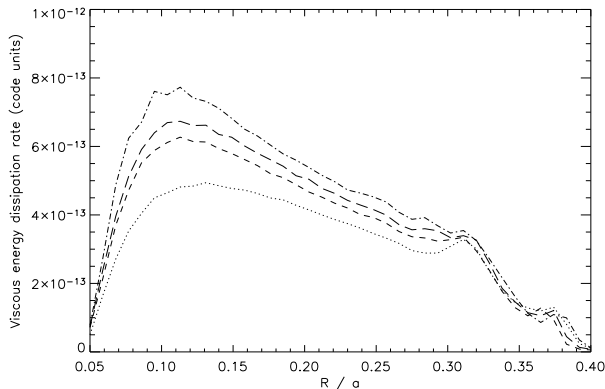


Figure 7. Evolution of total viscous energy dissipation rate in the second simulation. The lines correspond to the same times as those in Figure 6.

in dissipation in the outer disc brought about by the increasing surface density and central temperature is offset by the gradual cooling and shrinking of the high-viscosity inner region.

A steady increase in the mean brightness level between outbursts is unavoidable if the entire disc is in a single viscosity state, because both the surface density and temperature must be increasing. This has long been known to be the case from thermodynamically-detailed one-dimensional calculations in which the quiescent disc is entirely in the cool, low viscosity state. The effect of increasing Σ and T dominates the effect of the disc shrinking in quiescence (equation 7), and the brightness rises steadily.

However, we can see from equation 10 that this problem can be resolved if a small region remains in the high-viscosity state while the surface density and temperature increase in the rest of the disc. In the SPH calculations, this is achieved by the surface density hovering near the critical stability limit at all times. The high-viscosity, hot inner disc is the main difference between our simulations and those within the framework of the standard disc instability model (Lasota 2001), where the quiescent disc is cold everywhere and the surface density is left well below Σ_{\min} after each outburst.

The key question that will remain is how can this be achieved in a real accretion disc? It has been suggested that the inner parts of the accretion disc can be heated and evaporated near the white dwarf (Meyer & Meyer-Hofmeister 1994). Indeed, a low density region in the inner disc can explain the UV delay observed in dwarf novae, because at the onset of an outburst it takes a few hours for the low density region to refill. Of course, the UV delay will be present however the low density region arises: in addition to the evaporation model of Meyer & Meyer-Hofmeister (1994), Livio & Pringle (1992) have suggested that the inner part of a quiescent disc can be evacuated by the weak magnetic field of the white dwarf primary. An attractive feature of the models that we have presented in this paper is that a similar low-density inner disc is predicted during quiescence. Here, however, the small low density region is a consequence of a local viscosity higher than that which is usually assumed for a quiescent disc. This is exactly analogous to the situation found by Stehle & King (1998), who showed that the UV delay can be reproduced if irradiation by the hot white dwarf keeps the disc hot and fully ionised out to several stellar radii.

Although there are difficulties separating spectral components due to the accretion flow itself and the white dwarf in quiescent

dwarf novae, there is observational evidence to support the presence of such a hot, optically thin inner region (see, for example, la Dous et al. (1997); Done C. & Osborne J.P. (1997)). Such a flow would almost certainly be highly turbulent, and it is exactly these conditions under which the MRI is expected to be most efficient and the viscous stress high.

We conclude that the constant brightness level that is observed between the outbursts of dwarf novae is well explained by the gradual cooling of a small, critically-stable, hot inner region. The diminishing contribution to the viscous energy dissipation rate from such a region is sufficient to mask the increasing energy dissipation due to increases in mid-plane temperature and surface density in the rest of the cool disc.

ACKNOWLEDGMENTS

MRT acknowledges a PPARC Postdoctoral Fellowship.

REFERENCES

- Balbus S.A., Hawley J.F., 1991, *ApJ*, 376, 214
 Cannizzo J.K., Mattei J.A., 1992, *ApJ*, 401, 642
 Cannizzo J.K., Shafter A.W., Wheeler J.C., 1988, *ApJ*, 333, 227
 Done C., Osborne J.P., 1997, *MNRAS*, 288, 649
 Hameury J.-M., Menou K., Dubus G., Lasota J.-P., Huré J.-M., 1998, *MNRAS*, 298, 1048
 Ichikawa S., Osaki Y., 1992, *PASJ*, 44, 15
 la Dous C., Meyer F., Meyer-Hofmeister E., 1997, *A&A*, 321, 213
 Lasota J.P., 2001, *New Astronomy Reviews*, 45, 449
 Livio M., Pringle J.E., 1992, *MNRAS*, 259, L23
 Matsumoto R., Tajima T., 1995, *ApJ*, 445, 767
 Menou K., *Science*, 288, 2022
 Meyer F., Meyer-Hofmeister E., 1994, *A&A*, 288, 175
 Monaghan J.J., 1992, *ARA&A*, 30, 543
 Murray J.R., 1996, *MNRAS*, 279, 402
 Ritter H., Kolb U., 1998, *A&A*, 129, 83
 Shakura N.I., Sunyaev R.A., 1973, *A&A*, 24, 337
 Smak J., 1984a, *Acta. Astr.*, 34, 93
 Smak J., 1984b, *Acta. Astr.*, 34, 161
 Stehle R., King A.R., 1998, *MNRAS*, 304, 698
 Truss M.R., Murray J.R., Wynn G.A., Edgar, R., 2000, *MNRAS*, 319, 467
 Wagner R.M., Thorstensen J.R., Honeycutt R.K., Howell S.B., Kaitchuk R.H., Kreidl T.J., Robertson J.W., Sion E.W., Starrfield S.G., 1998, *AJ*, 115, 787
 Wood J., Horne K., Berriman G., Wade R., O'Donoghue D., Warner B., 1986, *MNRAS*, 219, 629